2ND QUARTERLY REPORT

NONDISSIPATIVE DC to DC REGULATOR-CONVERTER STUDY

15 September 1964 to 15 December 1964

Contract No.: NAS 5-3921

GPO PRICE $ _____

OTS PRICE(S) $ _____

Hard copy (HC) $3.00

Microfiche (MF) .50

Prepared by

Hamilton Standard DIVISION OF UNITED AIRCRAFT CORPORATION
ELECTRONICS DEPARTMENT BROAD BROOK CONN.

for

GODDARD SPACE FLIGHT CENTER
Greenbelt, Maryland

NONDISSIPATIVE DC TO DC REGULATOR-COVERTER STUDY

SECOND QUARTERLY REPORT

15 SEPTEMBER, 1964 to 15 DECEMBER, 1964

CONTRACT NO.: NAS 5-3921

GODDARD SPACE FLIGHT CENTER

GREENBELT, MARYLAND

Prepared by: E. Fruchter
E. Fruchter, Sr. Experimental Engineer

Approved by: W. Michel
W. Michel, Project Engineer

UNITED AIRCRAFT CORPORATION
HAMILTON STANDARD DIVISION
BROAD BROOK, CONNECTICUT

TABLE OF CONTENTS

(Continued)

LIST OF ILLUSTRATIONS

NASA STUDY

22549

I. ABSTRACT

The study during the second quarterly period included the following:

1. Magnetic study to determine frequency of operation.
2. Examination of pulse width variations necessary to control over total input range.
3. Examination of frequency variations necessary to control over total input range.
4. Examination of square wave sources.
5. Examination of power losses in saturated transformers.
6. Examination of various system concepts.
7. Selection of the system concept.
8. Initial examination of rectifying components.
9. Analysis of output filter section.

It was previously reported that the push-pull chopper and the push-pull inverter-rectifier were chosen as the basic circuits for further study.[7] It was further reported that a combination of pulse width and frequency modulation within the 20 to 30 KCPS range seemed to offer the most promising means of control.[7]

However, consideration of this study program's requirements to reduce the size and weight of all units as far as possible, and to minimize the use of magnetics, suggests that an investigation of digital circuits driving single-ended power stages is also in order. Means of synthesizing such systems were, therefore, also studied in this quarterly period.

An investigation of rectifying devices was conducted. Parameters effecting diode efficiency were examined, and the possibility of using germanium transistors as synchronous rectifiers was considered.

Finally, the stability of a choke input filter section and its response to various input waveforms was analyzed.

Author

II. PURPOSE

The purpose of this program is to provide concepts, techniques, and developed modular circuitry for non-dissipative DC to DC converters in the power range of 0 to 100 watts.

Major program goals are the maximization of efficiency, simplicity, and reliability, along with minimization of size, weight, and response times of the converters.

The circuits are to be modular in concept, so that a minimum of development is required to tailor a circuit to a specific application. The concepts should also allow, inasmuch as practical, for the use of state-of-the-art manufacturing techniques.

The program is multi-phased, including a study, analysis, and design phase, and a breadboard phase during which the concepts are to be verified by construction and test of eight breadboards.

III. INTRODUCTION

A magnetic study was conducted so as to establish the system's upper operating frequency. However, during this, the second quarterly period, the major portion of the effort was concerned with the conception of applicable control schemes. Methods for producing pulse width modulated, frequency modulated, and combination pulse and frequency modulated control systems were examined and an analysis of both pulse width and frequency modulation was performed to determine limits of operation.

An investigation of rectifying components and a stability analysis of the output filter section were also completed.

At this point, it is felt that although a stability analysis of the converter control circuits has not been conducted, breadboarding can begin on the premise that modifications will solve any stability problems that may arise.

IV. TECHNICAL DISCUSSION

A. Magnetic Study

As was previously reported[7], semiconductor efficiency appears to limit the upper frequency of system operation to about 30 KCPS. A series of toroidal transformer designs were generated to determine whether it would be possible to operate transformers efficiently under the same limitation. The toroidal configuration was chosen because of low leakage due to the uniformly distributed windings, and minimal acoustical noise.

The following table (Table I) was prepared for the output transformer of Figure 1 using the basic magnetic equation for square wave transformation (equation 1). The designs were based on the use of Indiana General type 0-5 material, a low loss ferrite.

$$N = \frac{E \times 10^8}{4 f B A_c} \qquad 1.)$$

Where; N = number of turns

E = required voltage

f = desired frequency

B = magnetic flux density

A_c = cross-sectional core area

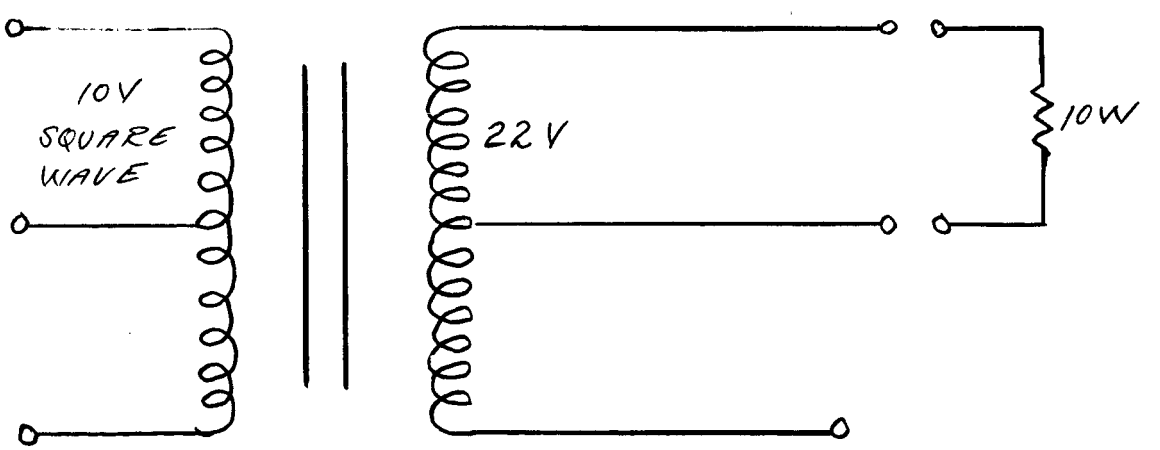

FIGURE 1. - 10 WATT OUTPUT TRANSFORMER

TABLE I - 10 WATT OUTPUT TRANSFORMER

	FLUX	COPPER	CORE		SIZE			
FREQ.	DENSITY	LOSS	LOSS	EFFICIENCY	O.D.	HEIGHT	VOLUME	NUMBER
10KC	2 Kg	.162W	.109W	97.3%	1.43"	.62"	.99"^{3}	F2070
10KC	1.5 Kg	.089W	.063W	98.6%	1.8"	.80"	2.05"^{3}	F-626-2
25KC	750 g	.143W	.04 W	98.2%	1.5"	.62"	1.0"^{3}	F2070
25KC	750 g	.05 W	.045W	99.1%	1.87"	.87"	2.4"^{3}	CF-113
50KC	2 Kg	.07 W	.208W	97.3%	.75"	.5"	.22"^{3}	F-846-3
50KC	500 g	.193W	.03 W	97.7%	1.37"	.62"	.915"^{3}	F-624-3
50KC	500 g	.065W	.072W	98.5%	1.37"	.62"	.915"^{3}	F-2070
50KC	500 g	.034W	.08 W	98.9%	1.62"	.62"	1.28"	CF-113

It is apparent from Table I above, that relatively efficient transformers of moderate sizes can be designed for operation to at least 50 KCPS. What is not apparent (and remained to be determined) is a definitive relationship among efficiency, weight, and frequency of operation.

General Electric, confronted with the same problem, developed the following analysis.[8]

The two principle sources of loss (core and winding losses) and the power rating of the transformers were expressed as functions of core geometry:

P_c = Core loss and is given by;

$$P_c = W(f,B)\ \delta_c\ A_c l_c \qquad 2.)$$

Where;

$W(f, B)$ = watts loss per pound of core material as a function of frequency (f) and flux density (B)

δ_c = effective density of the core material including insulation, space factor, binder, etc.

A_c = core cross sectional area

l_c = core mean length

P_W = winding loss and is given by;

$$P_W = \rho\ S\ J^2\ A_w l_m \qquad 3.)$$

Where, ρ = conductor resistivity

S = winding space factor (commonly = 0.4)

J = current density

A_W = area of core window allotted for winding

l_M = mean length of a winding turn

P_o = transformer power rating and is given by;

$$P_o = \sqrt{2}\ S\ f\ B\ I\ A_c A_W \qquad 4.)$$

Where, I = current flow in transformer secondary

Examination of equations 2, 3, and 4 indicates that core and winding losses vary as the cube of transformer dimensions ($A_c l_c$ and $A_W l_M$, respectively) while power rating varies as the fourth power of dimensions ($A_c A_W$). Therefore, as expected, an increase in the size of a transformer, with all other quantities held constant, will increase the efficiency of operation.

Efficiency will also be effected by the current density. Winding losses wil will increase as the square of current density while output power is directly proportional to this same parameter. Therefore, efficiency will ultimately be adversely effected. However, up to the point at which core and winding losses are equal, increasing current density will improve efficiency. In practice, even further increases may be desirable to improve light load operation and to attain a greater power output for a given design weight.

In order to establish a relationship between core and winding losses that will allow a selection of parameters to yield minimum weight or maximum efficiency, γ was defined as a proportionality constant:

$$\text{or;}\quad R_W = \gamma P_c \qquad 5.)$$

The relationships between core geometry, weight, and efficiency were then investigated.

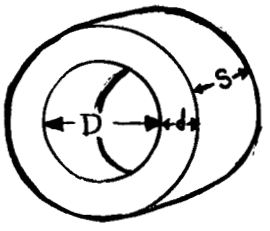

$$m = \frac{d}{D}$$

$$n = \frac{s}{D}$$

FIGURE 2. - TOROIDAL TRANSFORMER CORE

Considering Figure 2 above, the following may be determined:

$$A_c = sd = MN D^2 \qquad 6.)$$

$$A_w = \frac{3\pi}{16} D^2 \quad \text{(based on 3/4 of winding area being available for windings)} \qquad 7.)$$

$$\ell_c = \pi(D+d) = \pi(1+M)D \qquad 8.)$$

$$\ell_M = 2\left(\frac{\pi}{8}D + s + d\right) = 2\left(\frac{\pi}{8} + M + N\right)D \qquad 9.)$$

Neglecting mounting provisions, the weight of the transformer (M) is given by:

$$M = \delta_c A_c \ell_c + S\delta_w A_w \ell_M + (1-S)\delta_1 A_w \ell_M$$

or; $$M = \pi \delta_c \left[MN(1+M) + b\left(\frac{\pi}{8} + M + N\right)\right] D^3 \qquad 10.)$$

Where:

δ_c = equivalent density of the core material (including stacking factor)

δ_w = density of winding material

δ_1 = equivalent density of the insulation

S = winding space factor (commonly = 0.4)

$$b = \frac{3}{8}\left[\frac{S\delta_w + (1-S)\delta_1}{\delta_c}\right]$$

Typically, b might range between 0.1 and 0.4.

Substituting the expressions for core geometry into the power relationship yields:

$$P_c = \pi \delta_c W(f, B) MN(1+M) D^3 \qquad 11.)$$

$$P_w = \frac{3\pi}{8} S_\rho J^2 \left(\frac{\pi}{8} + M + N\right) D^3 \qquad 12.)$$

$$P_L = P_w + P_c = (1+\gamma) P_c \qquad 13.)$$

Where; P_L = combined core and winding losses

$$P_o = \frac{3\pi\sqrt{2}}{16} f B J MN D^4 \qquad 14.)$$

The function $[W(f, B)]$ may be expressed analytically as:

$$W(f,B) = fBH = \frac{fB^2}{\mu}\left(1 + j\,\frac{f}{f_o}\right) \qquad 15.)$$

Where: H = magnetic field strength

μ = permeability

$j = \sqrt{-1}$

f_o = critical frequency above which eddy current effects are applicable.

Equation 15 is valid for core materials in general. Some materials, however, exhibit a significant region in which the field strength is proportional to the half power of frequency due to skin effects within the core.

If these regions are not avoided, then the function W (f, B) must be altered for the particular material in question.

Using equation 15, the power relations of equations 11, 12, and 14, and the definition of γ (equation 5) expressions for weight and total losses were found to be:

$$M^8 = \pi^2\left(\frac{16\rho P_o^2}{3S}\right)^3\left(\frac{1}{\gamma^3}\right)\left\{\frac{\left[MN(1+M) + b\left(\frac{\pi}{B}+M+N\right)\right]^8\left[\frac{\pi}{B}+M+N\right]^3}{(MN)^9(1+M)^3}\right\}\left[\frac{\delta_c^5}{(fB)^6 W(f,B)^3}\right] \qquad 16.)$$

$$P_L^8 = \pi^2\left(\frac{16\rho P_o^2}{3S}\right)^3\left[\frac{(1+\gamma)^8}{\gamma^3}\right]\left[\frac{(1+M)^5\left(\frac{\pi}{B}+M+N\right)^3}{MN}\right]\left[\frac{\delta_c^5 W(f,B)^5}{(fB)^6}\right] \qquad 17.)$$

with the core diameter (D) required to give the desired output power determined as;

$$D^8 = \frac{16S\rho P_c^2\left(\frac{\pi}{B}+M+N\right)}{3\pi^2\gamma f^2 B^2 W(f,B) M^3 N^3 (1+M)} \qquad 18.)$$

FIGURE 3 - DIVISION OF LOSSES FOR A TRANSFORMER

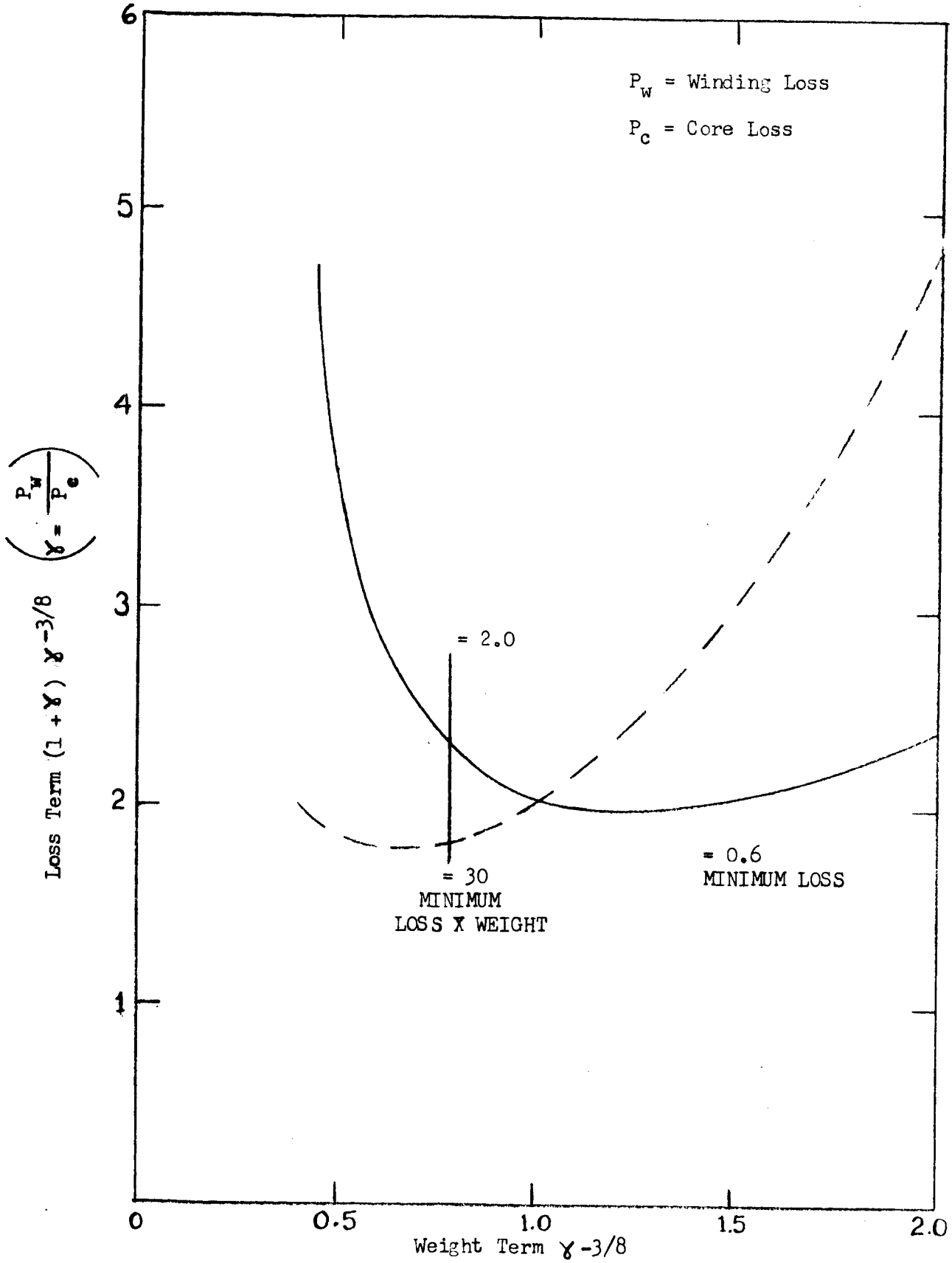

FIGURE 4 - CORE GEOMETRY

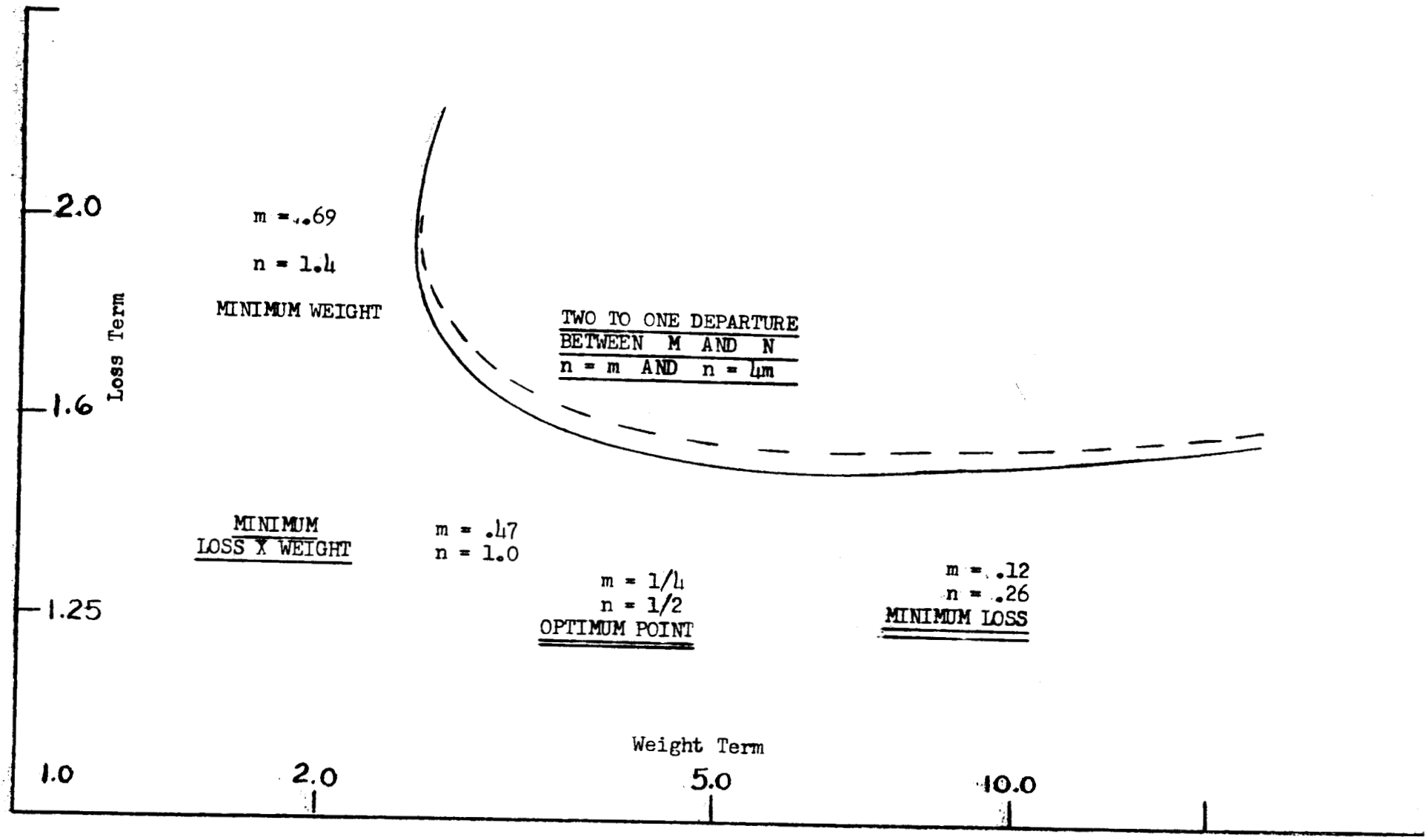

Previously, γ was defined as $\frac{P_L}{P_W}$. Figure 3 plots the loss determined function of γ versus the weight determined function of γ as defined in equations 16 and 17.

Clearly, from a weight standpoint γ should be held as large as possible while efficiency considerations indicate the reverse. Therefore, a practical range of γ was selected as follows:

$$\frac{3}{5} < \gamma < 3 \qquad 19.)$$

the upper limit being established at the minimum value of the product of weight and loss, while the lower was established at minimum loss.

For this possible five to one variation in γ, the weight and losses will vary as:

$$\frac{M_2}{M_1} = \left(\frac{1}{5}\right)^{3/8} = 0.547 \qquad 20.)$$

$$\frac{P_{L2}}{P_{L1}} = \frac{(1+3)}{(1+\frac{3}{5})}\left(\frac{1}{5}\right)^{3/8} = 1.37 \qquad 21.)$$

Similarly, in Figure 4, the loss and weight determined functions of m and n are plotted.

It turns out that the ratio between m and n is approximately one-half over the range of interest. However, altering this ration by a factor of two, will have no appreciable effect. The dashed curve of Figure 4 is appropriate for m = n, or for 4 m = n.

Placing limits on the excursion of m and n between the positions of minimum loss and minimum weight, a range is defined:

$$0.12 < m < 0.70 \qquad 22.)$$

$$0.25 < n < 1.40 \qquad 23.)$$

Within this range, weight and loss will vary as:

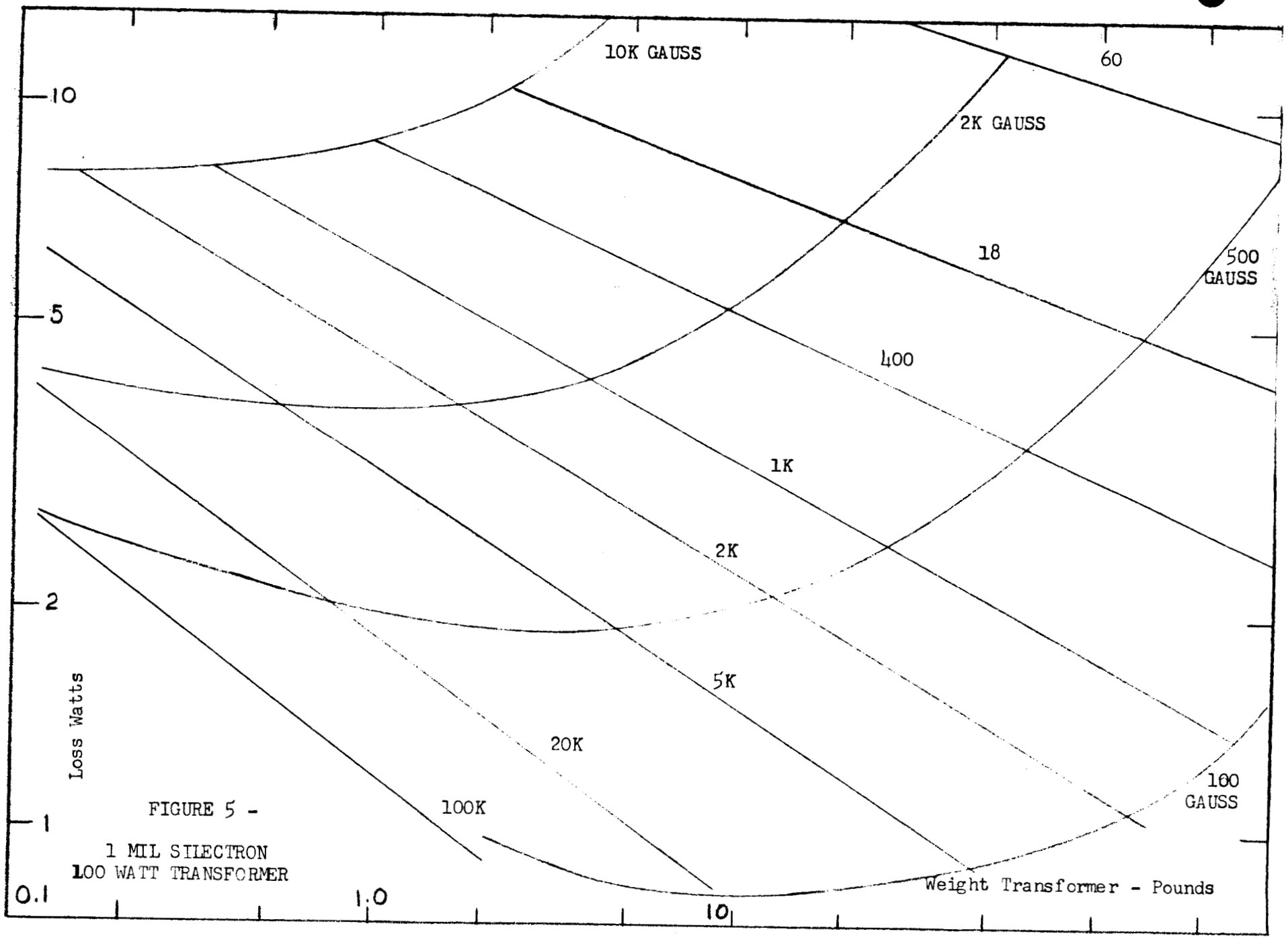

FIGURE 5 -

1 MIL SILECTRON
100 WATT TRANSFORMER

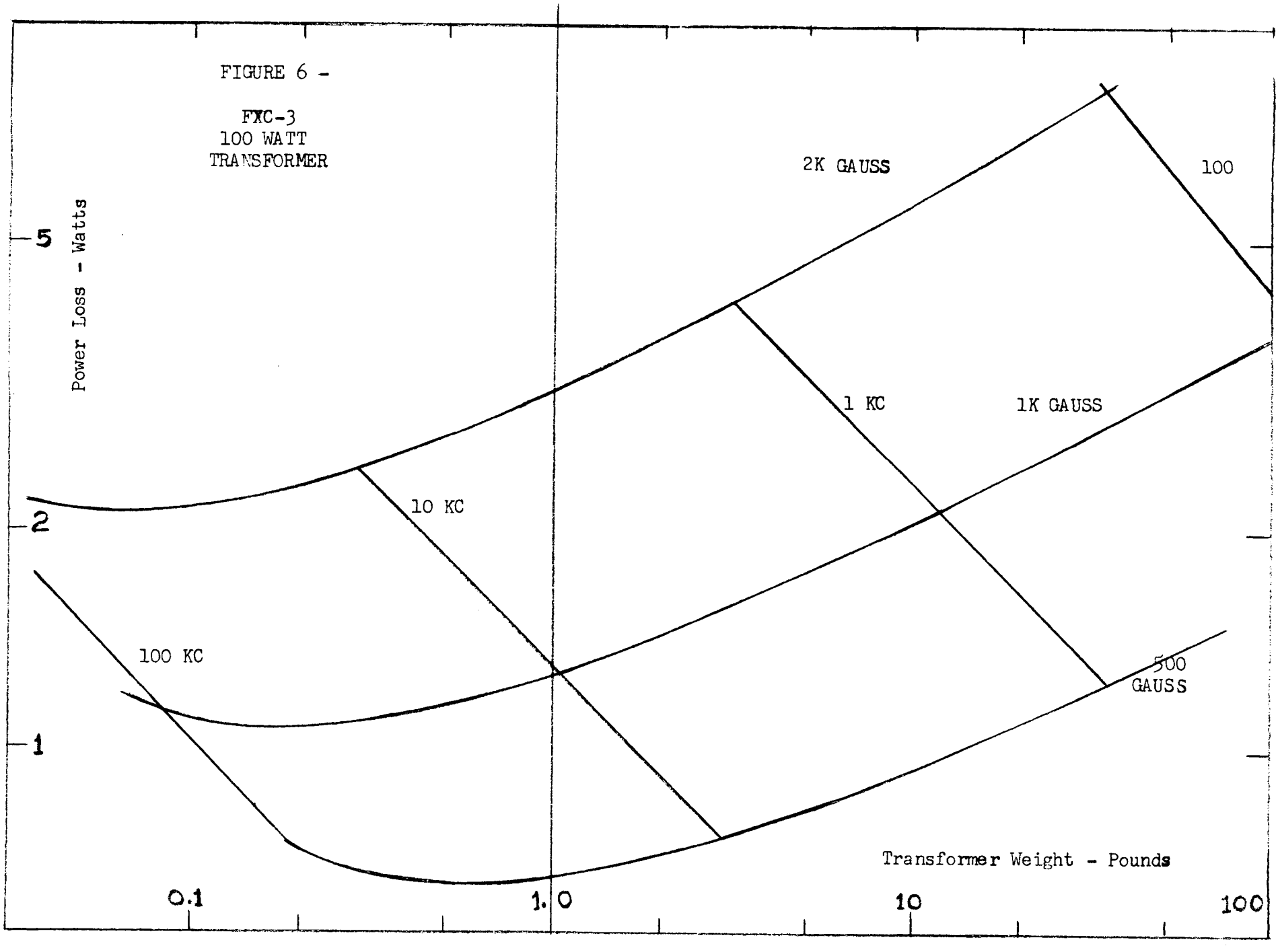
FIGURE 6 -
FXC-3
100 WATT
TRANSFORMER
Power Loss - Watts
5
2
1
2K GAUSS
100
1 KC
1K GAUSS
10 KC
100 KC
500
GAUSS
Transformer Weight - Pounds
0.1
1.0
10
100

$$\frac{M_2}{M_1} = 0.343 \qquad 24.)$$

$$\frac{P_{12}}{P_{11}} = 1.302 \qquad 25.)$$

Finally, using arbitrarily selected values of m, n, and γ (0.25, 0.50 and 2 respectively), curves of power loss versus weight were drawn. Because of the dependence of both weight and loss on the core properties and power output desired, Figures 5 and 6 represent two different situations. Each of them is drawn for a 100 watt transformer, but Figure 5 is drawn for 1 mil Silectron (a tape wound material) and Figure 6 is drawn for FXC-3 (a ferrite).

The use of these curves seems severely limited. However, in keeping with the three-quarter power relations between both losses and weight and transformer rating (Equations 16 and 17) the axis can easily be shifted according to the following:

$$\left(\frac{P_{o_1}}{P_{o_2}}\right)^{3/4} = K \qquad 26.)$$

Where; P_{o_1} = power rating desired

P_{o_2} = 100 watt power rating

K = shift factor

e.g. for a 10 watt transformer;

P_{o_1} = 10 watts

P_{o_2} = 100 watts

$$\left(\frac{P_{o_1}}{P_{o_2}}\right)^{3/4} = K = \left(\frac{10}{100}\right)^{3/4} = 0.18$$

Thus, values of power loss and weight, determined by the use of Figures 5 and 6, must be multiplied by 0.18 to be used for a ten watt design.

In a similar manner, changes in other design parameters can be accomodated, thus lending a universal character to these curves.

One other significant point should be mentioned, and that is: examination of these graphs clearly indicates the possibility of efficient transformer designs at reasonable weights throughout the 10 KCPS to 100 KCPS frequency range.

B. Pulse Width Modulation

A pulse width modulated system was assumed to be operating at 25 KCPS driving a pair of 2N2880 transistors in a push-pull configuration.

Maximum allowable pulse width was determined as follows:

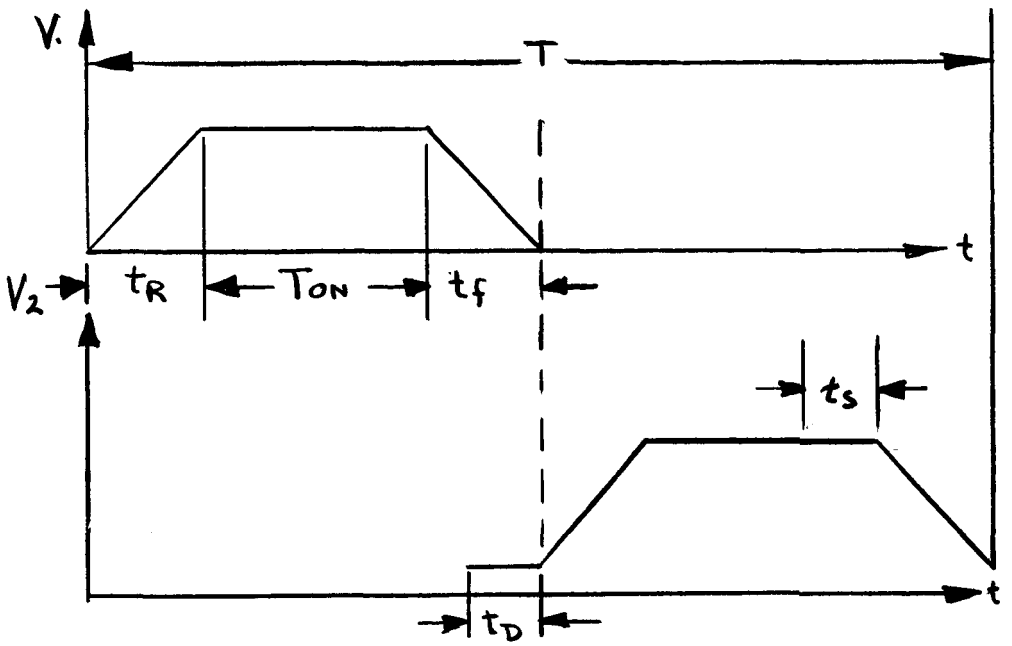

FIGURE 7. - OUTPUT WAVEFORMS OF PUSH-PULL STAGE

Referring to the above diagram, (Figure 7) it can be seen that the drive pulse width must allow for the transient characteristics of the transistor. The maximum allowable drive pulse width ($pw_{max.}$) is then determined as follows:

$$pw_{MAX} = \frac{1}{2} T - (t_s + t_f)_{Q_1} + (t_d)_{Q_2} \qquad 27.)$$

for the 2N2880:

ts = storage time $\cong$ 700NSEC

tf = fall time $\cong$ 300NSEC

td = delay time $\cong$ 20NS

than at 25KC:

$$pw_{max.} = \frac{1}{2}\left(\frac{1}{25\times10^{3}}\right) - (1.0\times10^{-6}) + (.02\times10^{-6})$$

$$pw_{max.} = 19.02\,\mu SEC.$$

Thus, to avoid entering into a condition where both transistors are in operation and the associated power losses are high, a margin of safety must be provided so that $pw_{max.}$ is not exceeded.

Considering the 10 watt regulator, we can compute the maximum and minimum pulse widths required as input voltage varies from 10 to 20 volts.

Where the output filter is considered ideal, the output voltage (Vout) is given by:

$$Vout = 2\left[\frac{V_M}{T}\left(T_{ON} + \frac{t_R + t_f}{2}\right)\right] \quad \text{which yields;}$$

$$T_{ON} = \frac{V_{OUT}\,T}{2V_M} - \frac{t_R + t_f}{2} \qquad 28.)$$

V_M = input voltage - collector/emitter saturation voltage

Or; $V_M = V_{IN} - V_{CE_{SAT}}$ 29.)

For 10 volt input:

Vout = 9 volts

V_M = 10 - .12 = 9.88 volts

$$\frac{t_R + t_f}{2} = 175 \times 10^{-9}$$

thus:

$$Ton = \frac{9\left(\frac{1}{25\times10^{3}}\right)}{2(9.88)} - 175\times10^{-9}$$

$$Ton = 18.08\,\mu SEC.$$

but:

$$pw = T_{ON} + (t_D + t_R) - t_S \quad (\text{FROM FIGURE 1}) \qquad 30.)$$

$$pw = 18.08\times10^{-6} + (20+50)\times10^{-9} - 50\times10^{-9}$$

$$pw = 17.35\,\mu SEC.$$

It is similarly found for the 20 volt input that:

$$pw = 8.25\,\mu SEC.$$

Thus, in order to control over the full input voltage swing the pulse width modulator must be capable of producing pulse widths that vary from 8.25 μsec to 17.35 μsec.

This in no way conflicts with the maximum allowable pulse width ($pw_{max.}$), nor does it impinge upon the unattainable requirements of either zero or infinite pulse widths.

It is then clear thatpulse width modulation is a plausible means of control.

C. Frequency Modulation

A frequency modulated system was assumed to be driving a pair of 2N2880 transistors in a push-pull configuration. Realizing that a maximum pulse width of 19.02 usec will produce a 50% duty cycle for each transistor at 25 KCPS, a pulse width of 15 μsec was selected so that the upper operating frequency would approach 30 KCPS. It should be noted that when an upper frequency is firmly established, one simply computes the maximum allowable pulse width as in IV B, above. In the discussion that follows, it was considered that the 15 μsec estimate made, somewhat arbitrarily, would be adequate.

Considering:

$$Vout = 2\left[\frac{V_M}{T}\left(T_{ON} + \frac{t_r + t_f}{2}\right)\right]$$

$$T = \frac{2V_M}{V_{OUT}}\left(T_{ON} + \frac{t_r + t_f}{2}\right) \qquad 31.)$$

But:

$$pw = t_D + t_r + T_{ON} - t_s \qquad 32.)$$

or;

$$Ton = pw + t_s - (t_r + t_D \qquad 33.)$$

Then:

$$T = \frac{2V_M}{V_{OUT}}\left[\left(pw + t_s + \frac{t_r + t_f}{2}\right) - (t_r + t_D\right) \qquad 34.)$$

Considering the 9 volt, 10 watt converter with input voltage variation from 10 to 20 VDC we find:

For 20 volt input;

$V_M = V_{IN} - V_{CE\,SAT}$

$V_M = 20 - 0.12 = 19.88$ VOLTS

then, $T = \frac{2(9.88)}{9}\left[(15\times10^{-6}+700\times10^{-9}+175\times10^{-9})-(70\times10^{-9})\right]$

$T = 69.85\,\mu SEC.$ (from Eq. 34)

$f = 14.32\,Kcps$

For 10 volt input;

$V_M = V_{IN} - V_{CE_{SAT}}$

$V_M = 10 - 0.12 = 9.88\,VOLTS$

then, $T = \frac{2(9.88)}{9}\left[(15\times10^{-6}+700\times10^{-9}+175\times10^{-9})-(70\times10^{-9})\right]$

$T = 34.71\,\mu SEC$ (from Eq. 34)

$f = 28.81\,Kcps$

The frequency modulation control device must then be capable of producing a driving function that varies in frequency between 14.32 KCPS and 28.8 KCPS. This driving function applied to the bases of the 2N2880 transistors would maintain regulation over the total input voltage range.

D. Square Wave Sources

A survey of possible square wave sources led to the following possibilities:

1. Saturating Cores Oscillators
   a. Single Transformer
   b. Dual Transformer
2. Relaxation Oscillator
   a. Unijunction Transistor
   b. Tunnel Diode
   c. Transistor
3. Multivibrator
   a. Astable
   b. Monostable
   c. Bi-stable
4. Schmidt Trigger
5. Clipped Sine Wave Oscillator

1. Saturating Core Oscillators

Both the single and dual transformer configurations of the basic saturating core oscillator were considered:

a. Single Transformer Saturating Core Oscillator

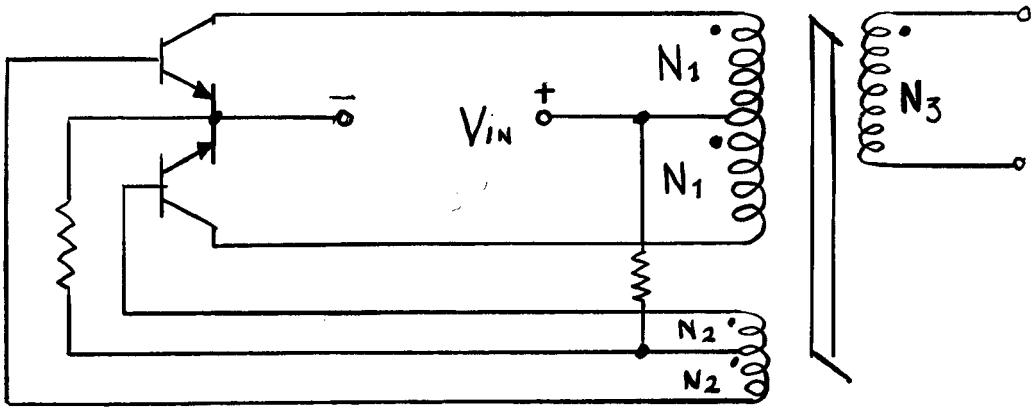

FIGURE 8. - SINGLE TRANSFORMER OSCILLATOR

The circuit illustrated (Figure 8) will produce a square wave output, the frequency of which is inversely proportional to input voltage.

Its disadvantages, the use of magnetics, and high power losses in the saturating output transformer, weigh heavily against its use.

b. Dual Transformer Saturating Core Oscillator

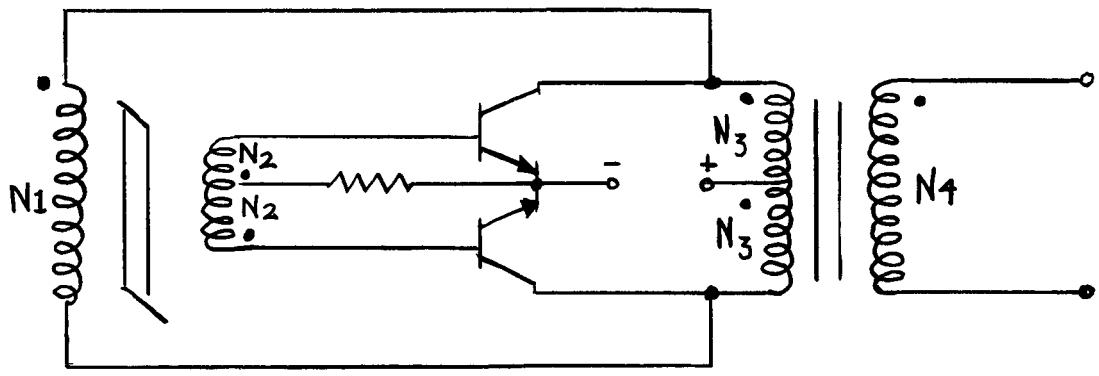

FIGURE 9. - DUAL TRANSFORMER OSCILLATOR

The above circuit (Figure 9) provides a square wave output at a frequency inversely proportional to input voltage. Power losses are minimized by not allowing the output transformer to saturate. The gain in efficiency is paid for by increased size and weight due to the use of additional magnetics.

2. Relaxation Oscillators

Three relaxation oscillators were considered; the unijunction transistor oscillator, the tunnel diode oscillator and the transistor oscillator using complementary symmetry.

a. Unijunction Transistor Relaxation Oscillator

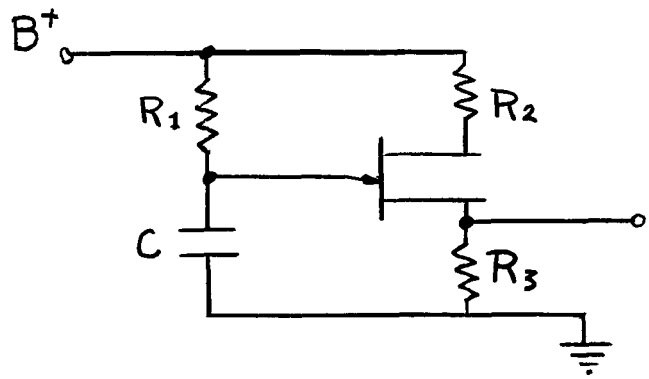

FIGURE 10 - UNIJUNCTION TRANSISTOR OSCILLATOR

The circuit shown above (Figure 10), has the attributes of great simplicity and ease of control. That is, since the frequency of oscillation is dependent upon the R_1 C time constant, replacing R_1, by a variable resistance, such as a transistor, will allow control over the circuit's output frequency.

b. Tunnel Diode Relaxation Oscillator

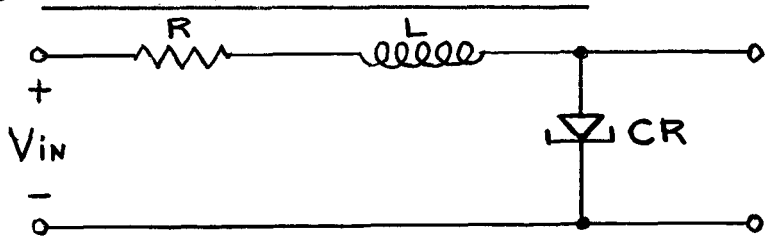

FIGURE 11 - TUNNEL DIODE OSCILLATOR

The simplicity of the tunnel diode relaxation oscillator (Figure 11) makes it highly attractive. However, its low level (millivolt range) operation makes it susceptible to noise, and its greates attribute of high speed (megacycle range) cannot be utilized.

c. Transistor Relaxation Oscillator

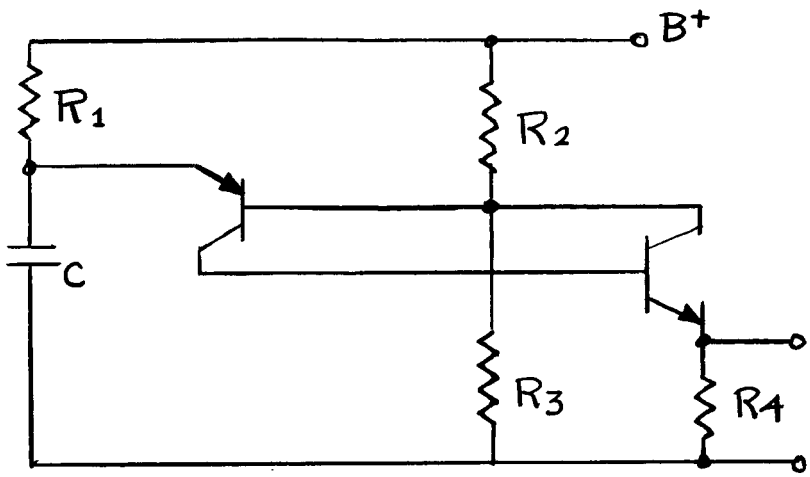

FIGURE 12 - TRANSISTOR OSCILLATOR

The use of complementary symmetry (Figure 12) produces an oscillator similar in operation to the unijunction transistor oscillator. The circuit is relatively simple and avoids the use of magnetics entirely.

Frequency variations can be produced by varying the R_1 C time constant. Thus, if R_1 is replaced by a transistor, the frequency of oscillation can be controlled by varying the base drive of this transistor.

The circuit does make use of a PNP device which makes it less economically attractive.

3. Multivibrators

The three classes of multivibrators were examined.

a. Astable Multivibrator

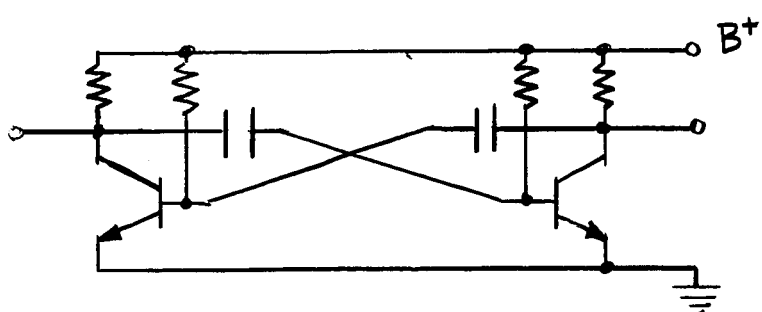

FIGURE 13 - ASTABLE MULTIVIBRATOR

The basic astable multivibrator, illustrated above (Figure 13), is somewhat more complex than any of the relaxation oscillators described. However, it does have interesting possibilities in a control application because the frequency of oscillation can be altered in several ways.

Changing B+, or either the base or collector resistance will change the output frequency. This suggests the possibility of using multiple control sources, and for the present application controlling with both input and output voltages can be an advantage.

b. Monostable Multivibrator

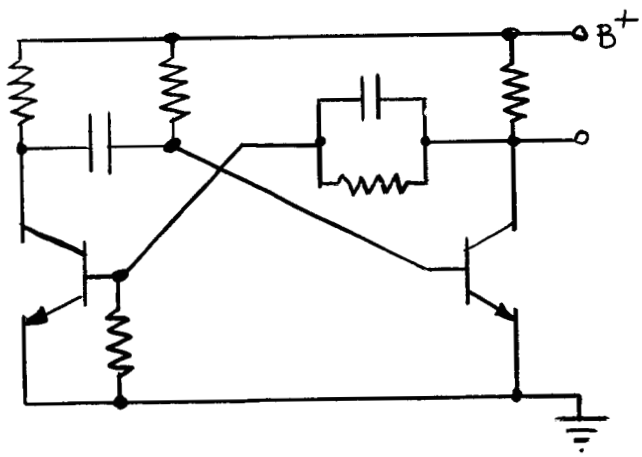

FIGURE 14 - MONOSTABLE MULTIVIBRATOR

The basic monostable (Figure 14) lends itself readily to a frequency modulated system due to the constant pulse width that it offers. In practice, however, it is often fairly difficult to maintain a constant pulse width over an operating frequency range under varying environmental conditions.

c. Bi-stable Multivibrator

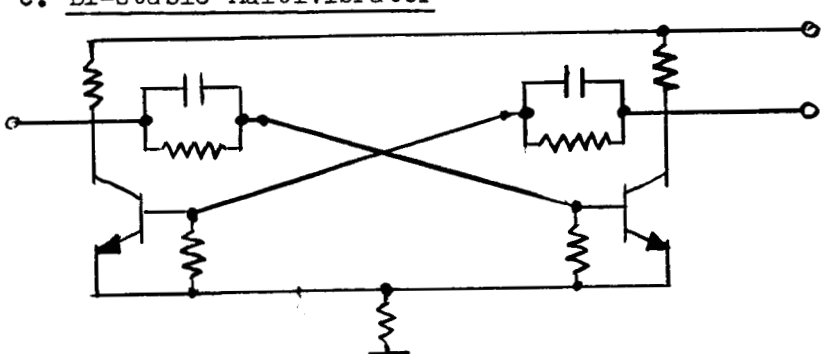

FIGURE 15 - BI-STABLE MULTIVIBRATOR

Of the circuits examined, the basic flip-flop, illustrated above (Figure 15), is most readily available in microminiature form. Keeping in mind the possibility of the future requirement for microminiaturized, modular circuitry, the flip-flops have a definite advantage.

However, a pulse source (for triggering) must be used in conjunction with the flip-flop andthis somewhat lessens the appeal.

4. Schmidt Trigger

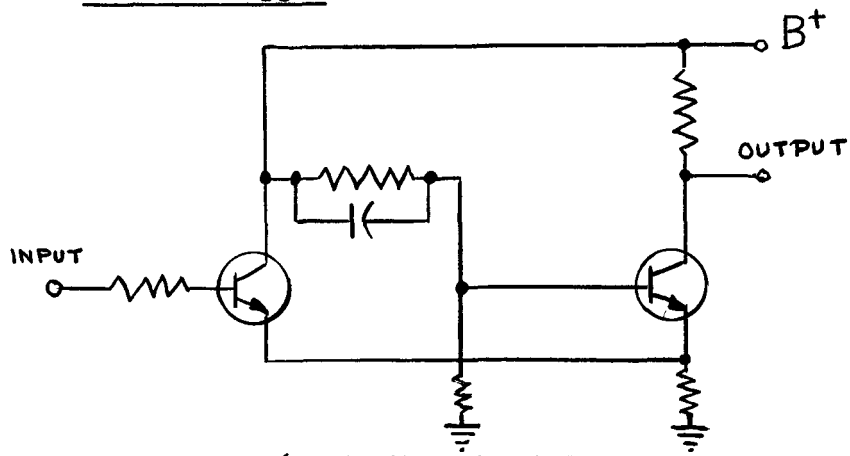

FIGURE 16 - SCHMIDT TRIGGER

The Schmidt Trigger (Figure 16) in conjunction with a repetitive ramp generator may be used as a square wave source. Modulation can be accomplished by varying the B^+ supply voltage.

Used as a square wave generator, the circuitry becomes a bit complex. However, the possibility of using the Schmidt trigger as a sensitive level sensor is still to be considered.

5. Clipped Sine Wave Oscillator

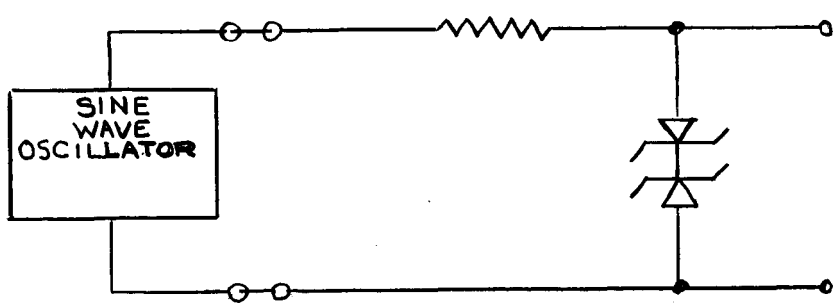

FIGURE 17 - CLIPPED SIME WAVE OSCILLATOR

A sinusoidal input voltage can be converted to a square wave by the clipping action of the zener diodes (Figure 17). It is required that the sinusoid's peak value be greater than the zener voltage, and the greater the difference, the more nearly square the output becomes.

Inherent in this means of producing square waves is a high power loss that is very unatrractive.

E. Power Losses in Saturated Transformers

The saturable core transformer, inherently, is a pulse width modulator. When driven by a variable frequency source, a system is formed that is capable of both pulse width and frequency modulation. This combined modulation scheme is attractive[7] and, therefore, the performance of the transformer was more closely examined.

A transformer was considered to be driving a pair of 2N2880 transistors into the saturation region:

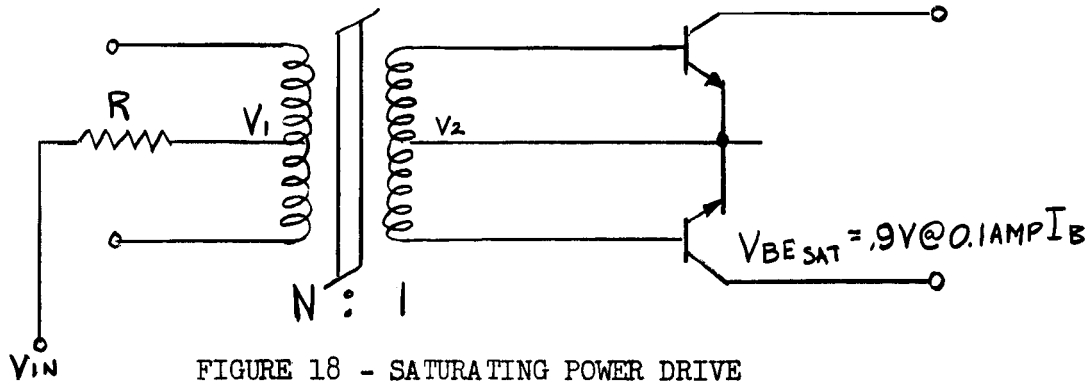

FIGURE 18 - SATURATING POWER DRIVE

The transformer was assumed at the edge of saturation at 10 volts input at 25 KCPS. It was then further assumed that Vin could increase to 20 volts, corresponding to the maximum input voltage of the 10 watt regulator. The following calculations were made to determine power losses in the transformer. Referring to the diagram above (Figure 18):

$$\frac{V_1}{V_2} = \frac{N}{1} \; ; \qquad \frac{I_1}{I_2} = \frac{1}{N} \; ; \qquad \frac{R_1}{R_2} = \frac{N^2}{1}$$

Neglecting core losses and transformer winding resistance; each half of the secondary circuit is reflected into the primary as a load equal to R_1.

$R_1 = N^2 R_2$ (where R_2 is the secondary load)

but;

$$R_2 = \frac{V_{BE}}{I_B}$$

then;

$$R_1 = \frac{V_{BE}}{I_B} N^2$$

Considering the voltage divider formed by R and R_1:

$$V_1 = \frac{V_{IN}\left(\frac{V_{BE}}{I_B} N^2\right)}{R + \left(\frac{V_{BE}}{I_B} N^2\right)}$$

or;

$$V_1 = \frac{V_{IN}}{1 + R/\left(\frac{V_{BE}}{I_B} N^2\right)} \qquad 35.)$$

but;

$$V_1 = N V_2 \qquad 36.)$$

and;

$V_2 = V_{BE\ SAT}$ (when transistor saturation is reached)

then;

$$N V_{BE_{SAT}} = \frac{V_{IN}}{1 + R/\left(\frac{V_{BE_{SAT}}}{I_B} N^2\right)} \qquad 37.)$$

or;

$$V_{BE_{SAT}} N^2 - V_{IN} N + I_B R = 0 \qquad 38.)$$

Solving for N;

$$N = \frac{V_{IN} \pm \sqrt{V_{IN}^2 - 4 I_B R V_{BE_{SAT}}}}{2 V_{BE_{SAT}}} \qquad 39.)$$

For N real:

$$V_{IN}^2 - 4 I_B R V_{BE_{SAT}} \geq 0 \qquad 40.)$$

or;

$$R \leq \frac{V_{IN}^2}{4 I_B V_{BE_{SAT}}} \qquad 41.)$$

An upper limit has then been established for R. R should be chosen as close to this limit as possible so as to hold saturation current to a minimum.

In the example that follows R is chosen equal to this upper limit.

$$R = \frac{V_{IN}^2}{4 I_B V_{BE_{SAT}}} \qquad \text{(from eq. 41)}$$

choosing worst case (Vin at minimum value);

$$R = \frac{10^2}{4(0.1)(0.9)}$$

$$R = 278\ \Omega$$

Solving for N;

$$N = \frac{10 \pm \sqrt{(10^2 - 4(1)(.9)278}}{1.8} \qquad \text{(from eq. 39)}$$

$$N = \frac{10 \pm 0}{1.8}$$

$$N = 5.56$$

A turns ratio of 5.5:1 is selected

Then:

During conduction at 10 volt input the primary current I_1 is found equal to:

$$I_1 = \frac{V_{IN}}{R + R_1} \qquad 42.)$$

$$I_1 = \frac{10}{278 + \left(\frac{V_{BE_{SAT}} N^2}{I_B}\right)}$$

$$I_1 = \frac{10}{278 + 272}$$

$$I = 18.1\ \text{MAMP.}$$

Constant power will be delivered throughout the cycle and thus primary power P_1 is equal to:

$$P_1 = I_1 V_{IN} \qquad 43.)$$

$$P_1 = 18.1 \times 10^{-3} (10)$$

$$P_1 = 181\ \text{MILLIWATTS}$$

At the 20 volt input level:

during transformer saturation:

$$I_{1\ max.} = \frac{V_{IN}}{R} \quad \text{(Since transformer action has ceased) 44.)}$$

$$I_{1\ max.} = \frac{20}{278}$$

$$I_{1\ max.} = 72\ MAMP.$$

Since the voltage has doubled, the constant volt-second nature of the transformer will lead to saturation during one-half of the cycle.

or:

$$P_{1\ sat.} = \frac{1}{2} I_{1MAX} V_{IN} \quad 45.)$$

$$P_{1\ sat.} = \frac{1}{2} (72 \times 10^{-3}) (20)$$

$$P_{1\ sat.} = 720\ MILLIWATTS$$

The problem remains to compute the primary circuit power losses during transformer conduction with 20 volts input: (Note: transistor saturation resistance assumed constant).

$$I_1 = \frac{V_{IN}}{R + R_1}$$

$$I_1 = \frac{20}{278 + 272}$$

$$I_1 = 36.2\ MAMP.$$

This power will be dissipated over half the cycle:

thus;

$$P_1 = \frac{1}{2} I_1 V_{IN}$$

$$P_1 = \frac{1}{2} (36.2 \times 10^{-3}) (20) \quad 46.)$$

$$P_1 = 362\ MILLIWATTS$$

Total power dissipated in the primary circuit with 20 volt input will then be:

$$P_{1\ av} = P_1 + P_{1\ SAT} \quad 47.)$$

$$P_{1\ av} = (362 + 720) \times 10^{-3}$$

$$P_{1\ av} = 1.08\ WATTS$$

The calculated losses are high. With the system delivering 10 watts, the loss of 1.08 watts represents a control loop efficiency of 90% which is not tolerable.

F. System Concepts

The following three concepts are shown with chopper power stages. It should be noted that similar systems driving inverter-rectifier power stages are realizable.

1. Pulse Width and Frequency Modulated Push-Pull Chopper

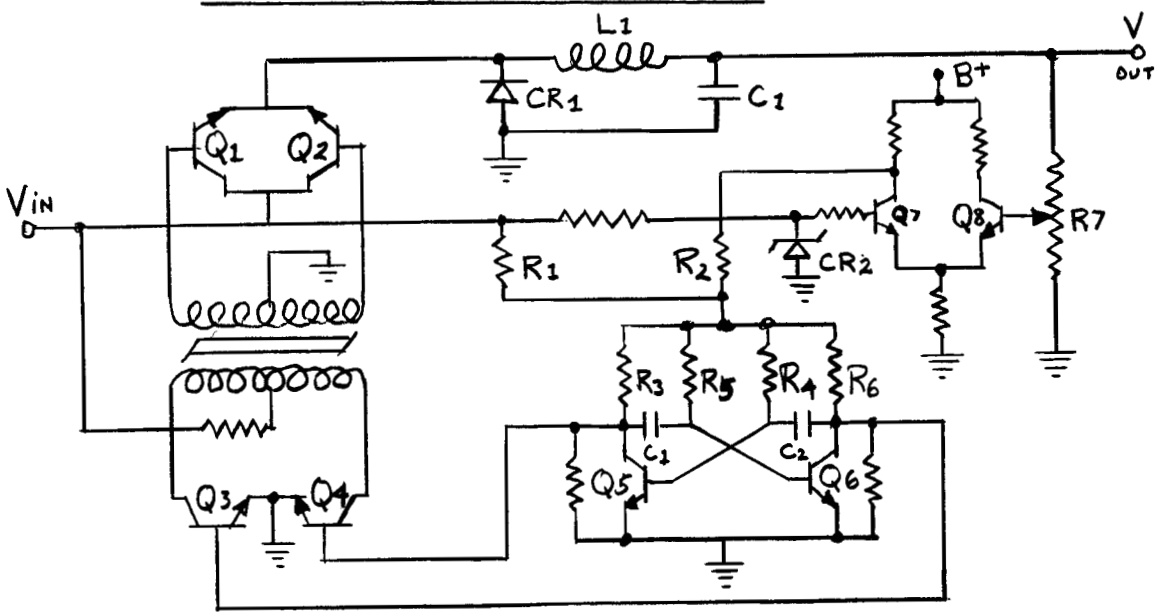

FIGURE 19 - PULSE WIDTH AND FREQUENCY MODULATED PUSH-PULL CHOPPER

a. Circuit Operation

Application of the input voltage, turns on the astable miltivibrator through starting resistor R_1. The multivibrator, formed by transistors Q5, Q6 and associated circuitry, provided square wave base drive to transistors Q3 and Q4.

This pair of transistors acts to invert the input voltage through the saturable transformer. The output of the transformer drives the bases of the chopper transistors Q1 and Q2 which produce the output waveform that is smoothed and filtered by CR1, L1 and C1.

Regulation is maintained by controlling both the frequency and pulse width of the chopper transistors' base drive in the following manner.

The differential amplifier formed by transistors Q7 and Q8 senses the difference between the reference voltage at the cathode of zener diode CR2 and the center tap of potentiometer R7. The difference signal, which is directly proportional to the output voltage, is added to the multivibrator bias level through resistor R2. The multivibrator bias becomes a function of both input and output voltage levels; being directly proportional to each. As the bias level is varied, the frequency of oscillation will vary as well.

Increasing the bias level causes the timing circuits formed by R3, R4, R5, R6, C_1 and C_2 to seek this higher level, and thus frequency is decreased. As voltage is decreased the reverse becomes true.

Pulse width modulation is effected by the action of the saturable transformer. The transformer is designed so that it reaches the saturation level when the input voltage is at a minimum. Thus, if the voltage rises, the transformer will shorten the pulse width to maintain a constant volt-second output.

b. Discussion

Several points should be noted:

First - Q3 and Q4 must provide enough amplification to drive the transformer. The operating level of the astable multivibrator must be kept low so that dissipation in the resistive elements is minimized. It is, therefore, possible that additional amplification between the multivibrator output and the transformer input will prove beneficial.

Secondly - the relationship between the astable multivibrator's frequency and bias level is logarithmic and not linear. If it is not possible to maintain control by placing narrow limits on frequency excursions, then other methods of controlling frequency can be considered. Among them, the use of additional transistors to vary effective timing resistance, or to control base drive current is most prevalent.

Finally, the transformer losses are relatively high. However, performance can be improved by the use of a self-stabilizing chopper circuit as described below.

2. Pulse Width and Frequency Modulated Self-Stabilizing Chopper

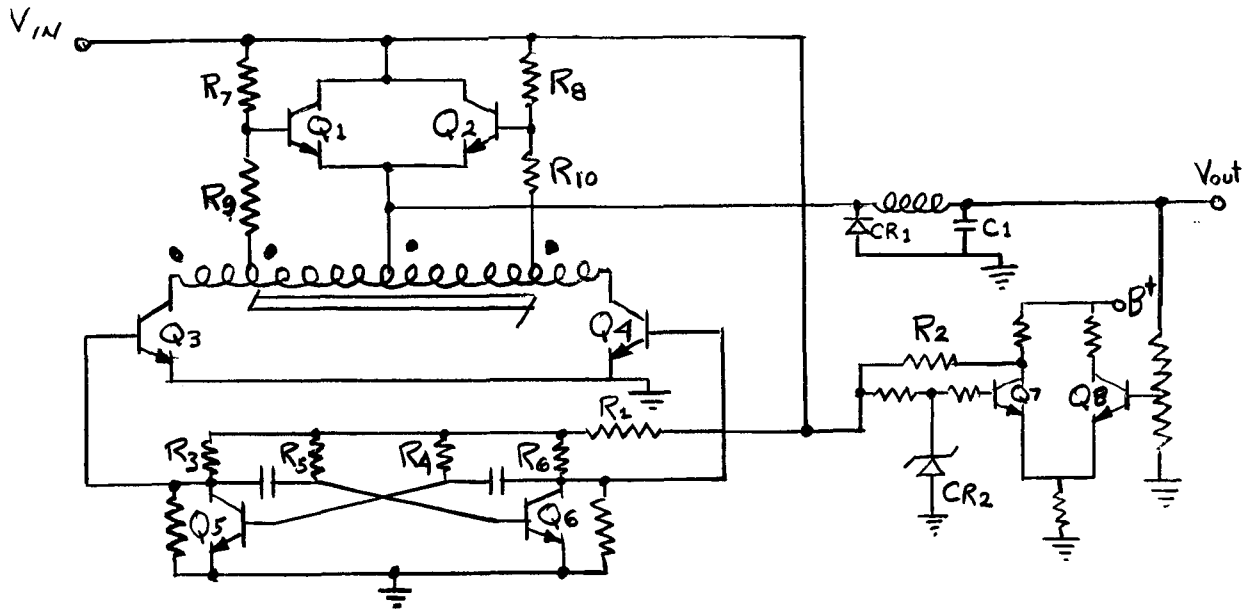

FIGURE 20 - PULSE WIDTH AND FREQUENCY MODULATED SELF-STABILIZING CHOPPER

a. Circuit Operation

The control and filter sections of the circuit illustrated above (Figure 20), are the same as those of the previously discussed concept. (Figure 19) It is in the power section that differences are apparent.

Consider a series of pulses being alternately applied to the bases of transistors Q3 and Q4. When the pulse is applied to Q3, the transistor will turn on and by autotransformer action, Q2 will be biased on. Transistor Q2 will remain on until the transformer saturates or is reset by the turning on of Q4. Turning on Q4 causes Q1 to be biased on, by the same autotransformer action, and Q4 remains on until either the transformer saturates, or until Q3 is once again turned on, resetting the transformer and completing a cycle.

The output of the chopper transistors Q1 and Q2 will then be pulse width modulated by the saturable transformer and dwell time will be established by the frequency of the driving function.

b. Discussion

The rather unique method of using the saturable transformer, conceived by A. Powell of HSD offers two distinct advantages:

First - the circuit is inherently short circuit proof since Q1 and Q2 are supplied with fixed base drive and regeneration cannot occur under short circuit conditions.

Second - Power losses during transformer saturation are reduced by the relatively high resistance of the starting resistors R7 and R8.

3. Frequency Modulated Single-Ended Chopper

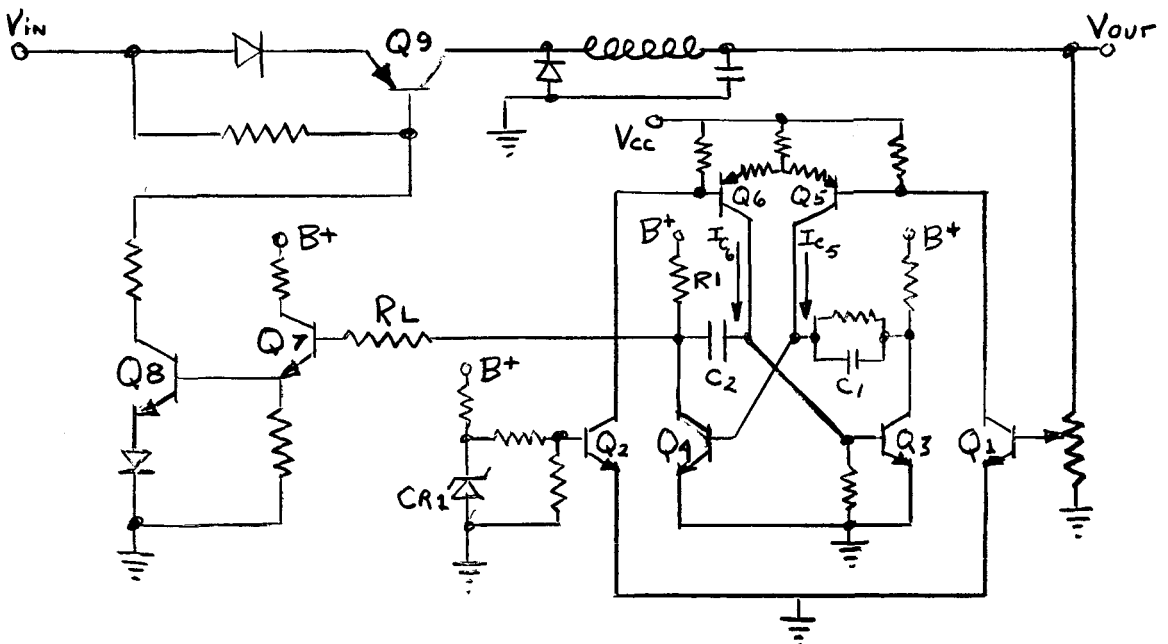

FIGURE 21 - FREQUENCY MODULATED SINGLE-ENDED CHOPPER

a. Circuit Operation

This circuit was presented in the April 1962 issue of Texas Instrument's Application Notes.[2] The differential amplifier formed by transistors Q1 and Q2 senses the difference between the reference voltage at the cathode of zener diode CR1 and the center tap of potentiometer R2. The output drives the second differential amplifier composed of Q5 and Q6.

The collector currents of Q5 and Q6 determined the circuit timing according to the following:

If t_1 = offtime of Q4 and t_2 = on time

then; $t_1 = \frac{V_{cc} C_1}{I_{c_5}}$ 48.)

$t_2 = \frac{V_{cc} \left(\frac{R_L}{R_L + R_1}\right) C_2}{I_{c_6}}$ 49.)

Examining the results of an increase in output voltage we find:

Q_1 begins to conduct more heavily;

The conduction of Q2 is lessened;

The voltage at the base of Q5 lowers, thus increasing I_{C_5} ;

The voltage at the base of Q6 raises, thus decreasing I_{C_6};

The net effect is then a shortening of transistor Q4 off time and a lengthening of Q4 on time.

It is also easily seen that a decrease in output voltage will cause the reverse effects.

Thus the frequency of the positive pulses seen by the driving transistors Q7 and Q8 is inversely proportional to output voltage and control of the chopper (Q9) is effected.

b. Discussion

This concept provides a means of control without the use of magnetics. In addition, the efficiency of 93% at 100 watts output as calculated by Texas Instruments[2] is attractive.

The problem of response time is not overcome, however. Sensing the output voltage and controlling on this one parameter limits the response time and does not provide the degree of control over input variations that is possible with the concepts previously discussed.

G. The System Concept

The system described in Section IV, F2 was chosen for further study. Its merits include the use of the push-pull power stage, previously determined[7] to be most suited to the present application.

It also makes use of a saturable transformer in the drive circuitry to pulse width control as a function of input voltage so as to improve response time. Although saturated magnetics are thus introduced, efficiency is held above the normal level by the circuit application.

The use of digital type circuits in the control loop was predicated on the anticipation that this would allow the easiest transition to a microminiaturized system. At the present time, low power, bi-stable multivibrators are available in off-the-shelf microminiature packages from several sources. It is possible, with present technology, to scribe the necessary resistors and capacitors on micro-wafers, to convert the bi-stable chips to astable units that are not presently available.

H. Rectifying Components

If total rectifier losses are considered to be forward power losses plus recovery power losses, (neglecting leakage effects) it is relatively easy to determine the rectifier parameter that most effects efficiency.

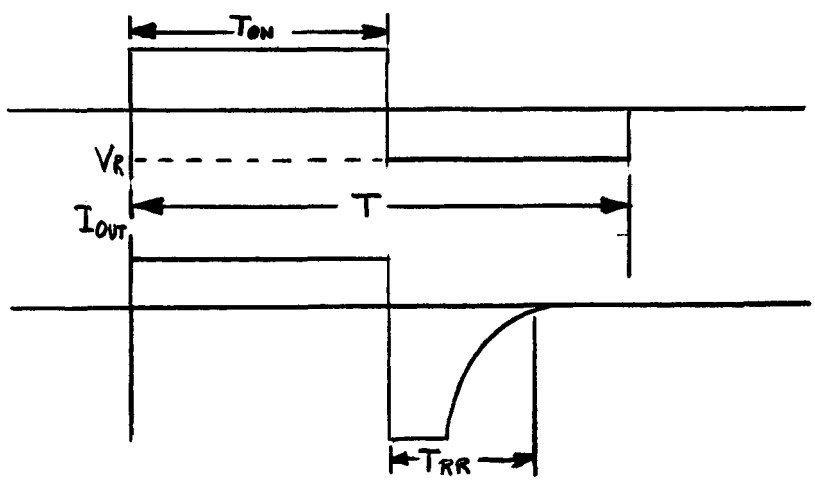

FIGURE 22 - SILICON DIODE OUTPUT WAVEFORM

P_f = forward power losses

$$P_f = \frac{1}{T}\int_0^{T_{ON}} V_f I_{OUT}\, dt \qquad 50.)$$

P_r = recovery power losses

$$P_r = \frac{1}{T}\int_0^{T_{RR}} V_R I_R(t)\, dt \qquad 51.)$$

Forward power loss is a function of the rectifier forward voltage, the load current drawn, and duty cycle. The two latter conditions are determined by external circuit requirements, while the forward voltage of silicon rectifiers, operating within specified limits, will not vary appreciably from unit to unit. Thus, the choice of rectifier will not significantly effect forward losses.

Considering recovery losses, it is found that a function of reverse voltage, reverse current, duty cycle, and reverse recovery time must be examined. Of these parameters, reverse recovery time (T_{RR}) is the only one that is primarily a function of rectifier design. The others are all primarily determined by external circuit conditions.

Thus, since power losses are directly proportional to reverse recovery time, and since only this parameter is basically a function of rectifier construction, then the choice of silicon rectifiers is narrowed to that unit which meets requirements imposed by circuit conditions, and that has the fastest recovery time.

Because of inherent low junction voltages, the use of germanium devices was also considered. However, germanium diodes are not readily available in the power ratings required and in the extensive Gulton Report[6], the use of germanium synchronous rectifiers is not recommended. It was deemed beyond the scope of the present program to explore this problem further.

I. Output Filter Section

The response of the following choke input filter was examined:

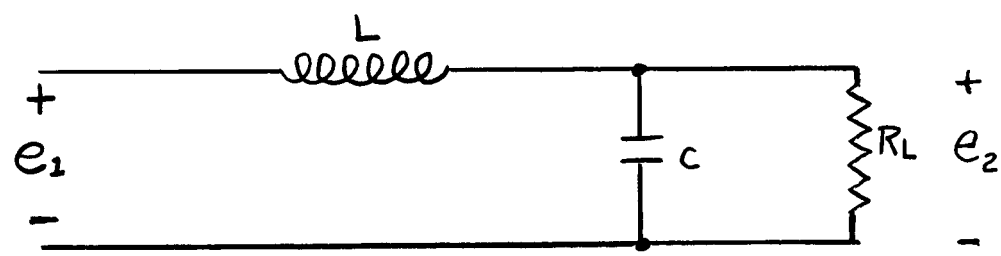

FIGURE 23 - CHOKE INPUT FILTER SECTION

1. The Filter Transfer Function

BY INSPECTION OF FIGURE 23:

$$E_2(P) = E_1(P)\left[\frac{\frac{R/cP}{R+1/cP}}{LP+\frac{R/cP}{R+1/cP}}\right]$$

$$E_2(P) = E_1(P)\left[\frac{1/LC}{P^2+\frac{1}{RC}P+\frac{1}{LC}}\right] \qquad 52.)$$

The transfer function, G_{12}, is;

$$G_{12} = \frac{E_2(P)}{E_1(P)} = \frac{1/LC}{P^2+\frac{1}{RC}P+\frac{1}{LC}} \qquad 53.)$$

or;

$$G_{12} = \frac{1/LC}{\left(P+\frac{1}{2RC}+\sqrt{\left(\frac{1}{2RC}\right)^2-\frac{1}{LC}}\right)\left(P+\frac{1}{2RC}-\sqrt{\left(\frac{1}{2RC}\right)^2-\frac{1}{LC}}\right)} \qquad 54.)$$

let; $\left[\frac{1}{2RC}+\sqrt{\left(\frac{1}{2RC}\right)^2-\frac{1}{LC}}\right] = a+jb$

and; $\left[\frac{1}{2RC}-\sqrt{\left(\frac{1}{2RC}\right)^2-\frac{1}{LC}}\right] = a-jb$

then;

$$G_{12} = \frac{1/LC}{(P+a+jb)(P+a-jb)} \qquad 55.)$$

Thus, the network has poles (maximum value of transfer function) at -(a+jb) and -(a-jb), and since the order of the denominator is two greater than that of the numerator, there are two zeros at infinity. The P plane plot of the transfer function G_{12} is, therefore:

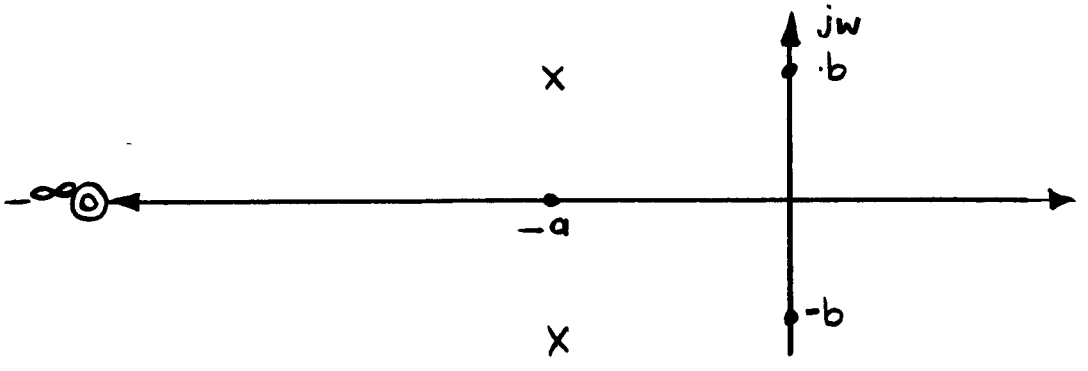

FIGURE 24 - "P" PLANE PLOT OF FILTER TRANSFER FUNCTION

The network is stable, since all poles of the transfer function have real parts which plot into the negative (left) half plane.

The denominator of equation 50. $\left(P^2 + \frac{1}{RC} P + \frac{1}{LC}\right)$

may be written as:

$$P^2 + \frac{1}{RC} P + \frac{1}{LC} = P^2 + 2\delta\omega_N P + \omega_N^2 \qquad 56.)$$

where ω_N = natural or undamped frequency expressed in radians/sec.

and δ = the damping ratio.

Assume a network where L = .8 mhy

C = 100 μf

R_L = 8 Ω (full load)

From equations 54 and 55, the poles may be determined as

$$(a+jb) = \frac{1}{2RC} + \sqrt{\left(\frac{1}{2RC}\right)^2 - \frac{1}{LC}} = 625 + j3480$$

$$(a-jb) = \frac{1}{2RC} - \sqrt{\left(\frac{1}{2RC}\right)^2 - \frac{1}{LC}} = 625 - j3480$$

If R_L is changed from 8Ω to 11Ω (3/4 load)

(a+jb) = 455 + j3500

(a-jb) = 455 - j3500

At 1/10 load, R_L = 80Ω and;

(a + jb) = 62.5 + j3540

(a - jb) = 62.5 - j3540

If the locations of the(a+jb) poles are plotted as a function of R_L, the following plot results:

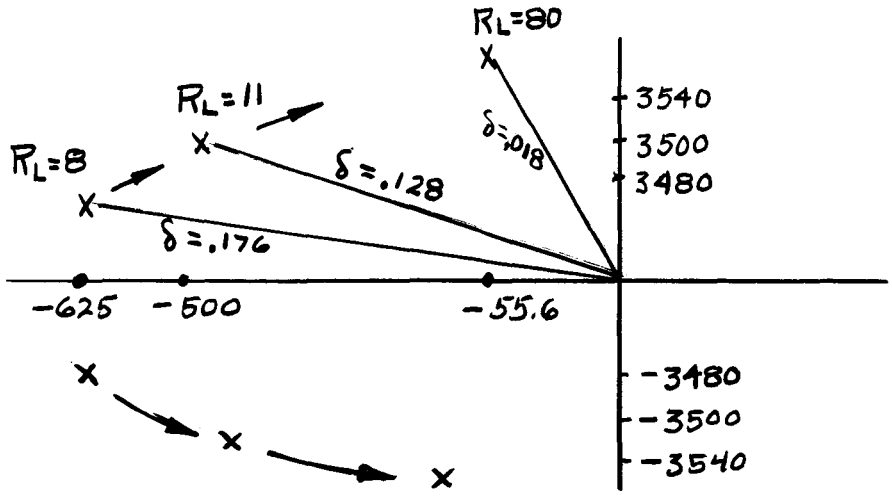

FIGURE 25 - "P" PLANE PLOT OF FILTER TRANSFER FUNCTION

Superimposed on the plot are contours of constant damping factor, δ. Thus it can be seen that, as R_L is increased, the filter's resonant frequency increases and the damping decreases. At R_L = ∞, the (a+jb) term will be purely imaginary and there will be no damping whatsoever, so that any input will result in an undamped sinusoidal oscillation. Thus, for this filter, no-load operation is impossible, and even at full load, the damping is so low that appreciable time would be required for any output oscillation to decay.

In order to achieve better damping and, thus, faster recovery, from equation 56.

$$\omega_N^2 = \frac{1}{LC} \quad \text{OR} \quad \omega_N = \sqrt{\frac{1}{LC}}$$

and; $2\delta\omega_N = \frac{1}{RC}$

therefore; $\delta = \frac{1}{2RC\omega_n} = \frac{1}{2RC\sqrt{1/LC}} = \frac{1}{2R(\sqrt{C/L})}$

An increase of δ requires a decrease of ω_N, $\sqrt{1/LC}$, OR $\sqrt{C/L}$

If δ is set to equal 0.8, and R_L = 8Ω, L = 0.8 Mhy;

$$\sqrt{C/L} = \frac{1}{2R\delta} = \frac{1}{2\times 8\times 0.8} = 0.078$$

and; $C = (0.078)^2 L \cong 5\mu f.$

If a minimum frequency of 20 KCPS is assumed, and the output ripple is to be 1%, then the choke impedance must be 99 x that of the capacitor at 20 KCPS, or

$$X_L = 99\, X_C:$$

$$\text{and;}\quad C = \frac{99}{\omega^2 L} \qquad 57.)$$

$$C = \frac{99}{(6.28\times 2\times 10^4)^2 (0.8\times 10^{-3})} = 7.2\,\mu f$$

Thus the requirement for a given ripple is slightly in conflict with the requirement for $\delta = 0.8$, but the difference is not great, so the 5 μf capacitor will be satisfactory here.

From equations 54 and 55, with L = .9 mhy, C = 5 uf, and R_L varied from 8Ω to 11Ω to 80Ω, the (a+jb) poles, and respective values of δ are:

R_L	a ± jb	δ
8Ω	12500±j9700	0.792
11Ω	9100±j12900	0.575
80Ω	1250±j15700	0.079

Thus, for step changes of load from 8 to 11 or 11 to 8 ohms, the use of a 5 μf rather than a 100 μf capacitor has greatly decreased the filter's transient recovery time but does so by sacrificing ripple attenuation to some extent. This network will still exhibit an undamped sinusoidal response at R_L=∞, however.

2. Consideration of Input Variations

For the 10 watt unit, the input voltage can vary between Vin min = 10V to Vin max = 20V, with 10MS rise and fall times, as shown:

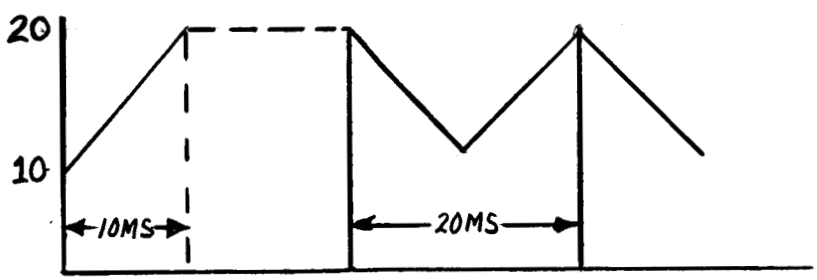

FIGURE 26 - SYSTEM INPUT VOLTAGE

In the worst case, if rise and falls follow each other immediately, the triangular portion could be represented, to a fair approximation, as a sinusoid. A single rise or fall is equivalent to a ramp.

For a fixed load, the power stage output (input to the filter) is a train of pulses, the width of each being proportional to the instantaneous amplitude of the input voltage, as shown:

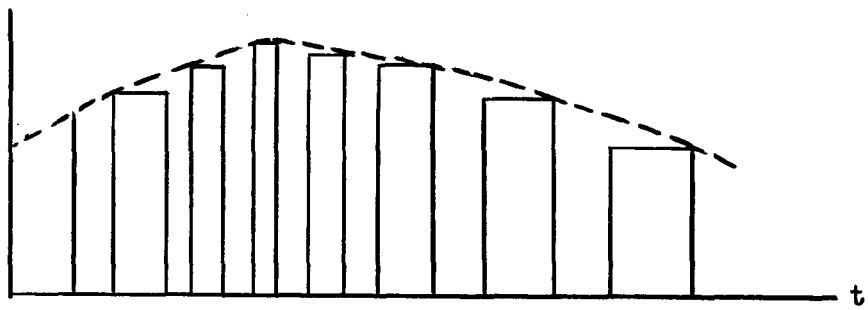

FIGURE 27 - POWER STAGE OUTPUT VOLTAGE

A continuous train of identical unit pulses can be represented by a Fourier series as;

$$f(t) = [\mu(t) - \mu(t-t_1)] + \mu(t-t_2) - \mu(t-t_2-t_1) + \cdots$$

$$f(t) = \sum_{\alpha=0}^{\infty} [\mu(t-\alpha t_2) - \mu(t-\alpha t_2 - t_1)] \qquad 58.)$$

The amplitude of a continuous train of identical unit pulses can be modulated by a sinusoid, as:

$$f'(t) = K f(t) \sin \omega t \qquad 59.)$$

but f(t) is in itself a function of the instantaneous value of sin wt, since the pulse width is varying inversely. It can readily be appreciated that the problem of calculating filter response to such an input is no easy task.

However, one may examine the response to individual portions of the input, such as a unit step, a unit ramp, and a unit sinusoid, in order to evaluate stability and behavior.

a. <u>For A Unit Step Input</u>: $E_1(P) = \frac{1}{P}$, and;

$$E_2(P) = E_1(P)\, G_{12} = \frac{1}{P} \frac{1/LC}{(P+a+jb)(P+a-jb)} \qquad 60.)$$

By Heaviside's expansion, this becomes:

$$E_2(P) = \frac{A}{P} + \frac{B_1}{P+a+jb} + \frac{B_2}{P+a-jb} \qquad 61.)$$

Since B1 and B2 are conjugates, $B_1 = Be^{-j\psi}$ and $B_2 = Be^{+j\psi}$

and;

$$e_2(t) = \mathcal{L}^{-1} E_2(P) = A + 2Be^{-at}\cos(bt+\psi) \qquad 62.)$$

Thus the output response is a constant voltage and a cosine term due to the poles of the transfer function, which decays with a time constant of 1/a. There is no instability evidenced, since there are no terms which increase indefinitely with time.

b. <u>For A Unit Ramp Input</u> $E_1(P) = \frac{1}{P^2}$, and;

$$E_2(P) = E_1(P)G_{12} = \frac{1}{P^2}\,\frac{1/LC}{(P+a+jb)(P+a-jb)} \qquad 63.)$$

$$E_2(P) = \frac{A}{P^2} + \frac{B}{P} + \frac{C_1}{P+a+jb} + \frac{C_2}{P+a-jb} \qquad 64.)$$

$$e_2(t) = \mathcal{L}^{-1} E_2(P) = At + B + 2Ce^{-at}\cos(bt+\psi) \qquad 65.)$$

The output is composed of the input ramp, a decaying cosine function, and an apparent constant voltage (B term), which can only be evaluated by an actual determination of coefficients. The output is again stable, however, since the only output function which increases with time is that the applied ramp itself.

c. <u>For A Unit Sinusoidal Input:</u> $E_1(P) = \frac{\omega}{P^2+\omega^2}$ and;

$$E_2(P) = \left(\frac{\omega}{P^2+\omega^2}\right)\frac{1/LC}{(P+a+jb)(P+a-jb)} \qquad 66.)$$

but; $\qquad (P^2+\omega^2) = (P+j\omega)(P-j\omega)$

therefore;

$$E_2(P) = \frac{\omega/LC}{(P+j\omega)(P-j\omega)(P+a+jb)(P+a-jb)} \qquad 67.)$$

$$E_2(P) = \frac{A_1}{P+j\omega} + \frac{A_2}{P-j\omega} + \frac{B_1}{P+a+jb} + \frac{B_2}{P+a-jb} \qquad 68.)$$

$$e_2(t) = \mathcal{L}^{-1} E_2(P) = 2A\cos(\omega t+\alpha) + 2Be^{-at}\cos(bt+\psi) \qquad 69.)$$

Thus, the output is the familiar decaying cosine term due to the poles of the transfer function, plus an undamped, phase shifted replica of the input sine function. Again, the response is stable because no terms increase with time.

3. Discussion

From consideration of load variations, the LC filter has the following characteristics:

1. It cannot be operated at no-load because at that condition, any input disturbance will result in a theoretically undamped oscillation at the LC resonant frequency.

2. For minimum recovery time the value of C is smaller than that necessary for a high degree of ripple attenuation.

The problem of describing, mathematically, the actual input to the LC filter is quite difficult. However, at load conditions other than no-load, the response of the filter is stable for any recognizable component of the input, namely, unit steps, ramps, and sinusoids. Therefore, in the open loop condition, it should be stable.

V. CONCLUSIONS AND RECOMMENDATIONS

The magnetic study conducted indicated the plausibility of efficient transformer operation throughout the frequency range from 10 to 100 KCPS. Therefore, an upper frequency limit of 30 KCPS will be imposed due to the semiconductor limitations previously discussed.

Furthermore, it has been shown mathematically that either pulse width or frequency modulation can be used in the control loop, Hoever, in order to improve response time, a combination of the two will be attempted. The saturating core transformer will be used to adjust the driving pulse width as a function of input voltage, while load variations will be compensated for by drive frequency adjustments.

The self-stabilizing circuit, conceived by A. Powell of Hamilton Standard Division, will be used in the power drive circuitry so as to reduce the high losses of the saturated transformer. The frequency of the control multivibrator will be adjusted by varying the transistors' base current. This will be accomplished by either controlling the bias voltage level or by using additional transistors to control resistance in the multivibrator's timing circuits.

The examination of rectifying devices has led to the selection of the silicon diode. The possible use of germanium units was ruled out because of the unavailability of germanium diodes capable of handling the power requirements, and because extensive work by Gulton Industries[6] indicated that germanium transistors would not be suitable as synchronous rectifiers.

Finally, the analysis of the choke input filter led to the conclusion that the open loop response of the circuit would be stable. The analysis also revealed that there would be no damping under no load conditions. It is expected, however, that the inherent resistance found in the inductor and capacitor will provide tolerable damping.

VI. PROGRAM FOR NEXT INTERVAL

During the next quarterly period, effort will be directed to the following areas:

A. Overall circuit concept; a detailed circuit concept of one regulator will be generated.

B. Preliminary breadboard work; control circuits, power stage, and output filters will be breadboarded to check out the circuit concept and to investigate the short circuit and transient recovery.

C. Detail Design; detailed designs of the seven remaining regulators will be initiated.

VIII. NEW TECHNOLOGY

It is possible that the power drive circuitry selected for further study will be an advance in present technology. However, circuit development efforts must be expended before conclusions can be drawn.